vices; to fabricate 3D computational devices, we must incorporate elements of digital logic [e.g., five-pin, single-logic gates (*19*)]. Self-assembly facilitates the formation of highly interconnected elements in both deterministic and probabilistic networks; it may be possible to use this kind of self-assembly to generate other logical structures (e.g., artificial neural networks) (*20*).

We have carried out all experiments using only a limited number of polyhedra: to extend this approach to a larger number of elements, and to smaller elements, it will be necessary to develop practical methods for fabricating these elements; the need for 3D microfabrication permeates 3D self-assembly, but new methods are beginning to emerge (*21–24*). Although large arrays may have defects, it may be possible to develop computational algorithms even in defective networks (*25–28*).

References and Notes

1. S. A. Campbell, *The Science and Engineering of Microelectronic Fabrication* (Oxford Univ. Press, New York, 1996).
2. S. K. Gandhi, *VLSI Fabrication Principles* (Wiley, New York, ed. 2, 1994).
3. W. Maly, *Atlas of IC Technologies: An Introduction to VLSI Processes* (Benjamin-Cummings, Menlo Park, CA, 1987).
4. P. M. Zavracky, M. Zavracky, V. Duy-Phach, B. Dingle, U.S. Patent 5,976,953 (1999).
5. H. J. Yeh and J. S. Smith, *IEEE Photonics Technol. Lett.* **6**, 706 (1994).
6. C. D. Fung, P. W. Cheung, W. H. Ko, D. G. Fleming, Eds., *Micromachining and Micropackaging of Transducers* (Elsevier, Amsterdam, 1985).
7. J. W. Sliwa Jr., U.S. Patent 5,075,253 (1991).
8. T. L. Breen, J. Tien, S. R. J. Olivier, T. Hadzic, G. M. Whitesides, *Science* **284**, 948 (1999).
9. L. F. Miller, *IBM J. Res. Dev.* **13**, 239 (May 1969).
10. R. R. A. Syms and E. M. Yeatman, *Electron. Lett.* **29**, 662 (1993).
11. F. K. Harsh, V. M. Bright, Y. C. Lee, *Sens. Actuators A* **77**, 237 (1999).
12. Masters for forming the polyhedra were machined out of aluminum, and molds were made from these masters using poly(dimethyl siloxane) (PDMS Sylgard 184, Dow Corning). Polymeric polyhedra were then cast in these molds, using a photocurable polymer (NOA 73, Norland). A sheet of flexible copper-polyimide composite (Pyralux LF 9110, DuPont) was coated with a photoresist (Microposit, 1813, Shipley), using hexamethyldimethylsiloxane (HMDS) as a primer. Both were spun on at 4000 rpm. After a soft-bake at 115°C for 5 min, this sheet was exposed to UV light through a negative mask containing an array of the pattern of connector dots, contact pads, and wires. The exposed photoresist was developed, and the exposed copper was removed by etching with an aqueous ferric chloride solution (1.4 g of $FeCl_3$ per milliliter of H_2O). Unexposed photoresist was removed with acetone. The basic pattern was then cut out manually and glued (Krazy Glue, Elmer's Products) to the faces of the polyhedra. In the demonstrations of parallel and serial networks, LEDs (BL-HS136, American Bright Optoelectronics) were manually soldered (Rosin Core Solder, Radio Shack, m.p. ~185°C) onto the copper contact pads. These soldered regions were coated with a thin impervious layer of adhesive (CA-50 Gel, 3M) to avoid wetting and cohesion of these regions during assembly. The adhesive was allowed to harden completely over 48 hours. The polyhedra were then immersed in a bismuth solder (117, Small Parts Inc., m.p. ~47°C), which was melted in an aqueous solution of hydrochloric acid (pH ~ 1). The acid dissolved the oxide layer on the copper and the solder. The solder coated only the exposed copper regions on the polyhedra (dots and wires), but did not wet the polymeric surfaces. The solder-coated polyhedra were allowed to self-assemble in an aqueous KBr solution [density of 1.1 to 1.4 g/cm^3, pH of 3 to 4, adjusted with acetic acid to dissolve oxides on the solder (a function similar to that of flux in conventional soldering) and ~0.001% (v/v) of detergent (Triton X-100, Aldrich) to prevent the formation of bubbles at the surface of the polyhedra] in an indented round-bottomed flask, heated above the melting point of the solder (~70°C) in an oil bath. The flask was placed horizontally on a rotary evaporator that was rotated at 5 to 20 rpm. All self-assemblies were complete within 1 hour. The assemblies were rotated for an average of 15 min after they formed, at which time the assembly was allowed to cool. We believe that the last 15 min may serve to anneal the structure to correct errors in the connections. On cooling, the molten solder interconnections solidified and gave the aggregates sufficient strength so that they could be manipulated.
13. Two electrically isolated wires connected the two sets. An LED was soldered on the contact pads between the wires, using a polarity in which the cathode was connected to the wire between dots {2, 5, 8, and 11}, and the anode was connected to the wire between dots {1} (Fig. 3A). The pattern was glued on the TO in such a way that the copper dots covered two opposite square faces, while the two wires ran across the two hexagonal faces between them.
14. In order to reduce the number of circuits that would be formed (and of LEDs required to check their electrical connectivity) and to minimize the geometrical problems of packing the LEDs in the arrays, only four of the dots (we call these dots "active") in the solder pattern ({3, 9} and {7, 13}) were wired to LEDs. The other four dots ({6, 12} and {4, 10}) in the pattern were connected to each other (we call these dots "passive"). A single TO contained eight LEDs, one on each of the hexagonal faces, with the square faces covered with the pattern of connector dots. The active and passive dots had twofold symmetry, while the global pattern on individual connector dots on the assembling square faces had fourfold symmetry. This difference in symmetry resulted in the formation of a stochastic network upon self-assembly [if a deterministic network were required, all the dots ({3, 6, 9, and 12} and {4, 7, 10, and 13}) would need to be connected to LEDs]. There are three types of connections which result from overlap of dots at each assembling face: (i) connections between LEDs on different TOs, involving only active dots with a probability of one-fourth; (ii) connections between LEDs on the same TO, involving both active and passive dots with a probability of one-half; and (iii) connections containing no LEDs, involving only passive dots with a probability of one-fourth.
15. In a bipolar, random system, the probability of the anode connecting to the cathode is one-half. For 10 LEDs to form a functional serial loop, the probability would be $1/2^9$ or 1/512.
16. I. S. Choi, N. Bowden, G. M. Whitesides, *Angew. Chem. Int. Ed. Engl.* **38**, 3078 (1999).
17. N. Bowden, A. Terfort, J. Carbeck, G. M. Whitesides, *Science* **276**, 233 (1997).
18. P. W. Rothemund, *Proc. Natl. Acad. Sci. U.S.A.* **97**, 984 (2000).
19. Five-pin, single-logic gates are part of the "Little Logic" line of products sold by Texas Instruments.
20. M. H. Hassoun, *Fundamentals of Artificial Neural Networks* (MIT Press, Cambridge, MA, 1995).
21. J. Tien, T. D. Clark, D. Duffy, G. M. Whitesides, in preparation.
22. Y. Yin, B. Gates, Y. Xia, *Adv. Mater.*, in press.
23. R. R. A. Syms, *J. Microelectromech. Syst.* **8**, 448 (1999).
24. A. Ishikawa, U.S. Patent 6,069,682 (2000).
25. J. J. Hopfield and D. W. Tank, *Science* **233**, 625 (1986).
26. C. Mead, *Proc. IEEE* **78**, 1629 (1990).
27. P. D. Tougaw and C. S. Lent, *J. Appl. Phys.* **75**, 1818 (1994).
28. J. R. Heath, P. J. Kuekes, G. S. Snider, R. S. Williams, *Science* **280**, 1716 (1998).

29. Supported by Defense Advanced Research Projects Agency/SPAWAR/AFRL and the NSF (CHE-9901358 and ECS-9729405). We thank S. Brittain for help with photography.

21 April 2000; accepted 22 June 2000

A [2]Catenane-Based Solid State Electronically Reconfigurable Switch

Charles P. Collier, Gunter Mattersteig, Eric W. Wong, Yi Luo, Kristen Beverly, José Sampaio, Françisco M. Raymo, J. Fraser Stoddart,* James R. Heath*

A solid state, electronically addressable, bistable [2]catenane-based molecular switching device was fabricated from a single monolayer of the [2]catenane, anchored with phospholipid counterions, and sandwiched between an n-type polycrystalline silicon bottom electrode and a metallic top electrode. The device exhibits hysteretic (bistable) current/voltage characteristics. The switch is opened at +2 volts, closed at −2 volts, and read at ~0.1 volt and may be recycled many times under ambient conditions. A mechanochemical mechanism for the action of the switch is presented and shown to be consistent with temperature-dependent measurements of the device operation.

Modern molecular electronics began in 1974 when Aviram and Ratner (*1*) proposed a molecular rectifier based on an asymmetric molecular tunneling junction. As various synthetic and analytical tools have been developed, it has become possible to contemplate a real technology based on molecular electronic devices. Several fundamental devices using molecules have recently been demonstrated, including rectifiers (*2*), resonant tunnel junctions (*3*), and singly settable molecular switches that can be electronically configured for wired-logic gates (*4, 5*). In this report, we describe a reconfigurable molecular-based solid state switch capable of ambient operation. The device was fabricated from a single

monolayer of a bistable [2]catenane (*6*–*8*) that was anchored with amphiphilic phospholipid counterions and sandwiched between an n-type polycrystalline Si (poly-Si) electrode and a Ti/Al top electrode. The device exhibits hysteretic (bistable) current/voltage characteristics. The switch can be opened at +2 V, closed at −2 V, and read between 0.1 and 0.3 V and may be recycled many times.

The standard switch of integrated circuit technology is the three-terminal Si-based transistor. Such devices are not just switches—they can also exhibit gain. Our long-term goal is to construct prototype electronics circuits by using bottom-up (chemical assembly) manufacturing (*9*). Because chemical assembly results in periodic structures, it is difficult to imagine how three-terminal devices can be made to tile a two-dimensional surface. Thus, our approach is to separate the function of gain from that of switching and thereby open up the possibility of two-terminal switching devices, which are amenable to chemical assembly. For a two-terminal switch, the various tasks of opening, closing, and interrogating the switch may be accomplished by using different voltages. An analogy is a magnetic bit that is characterized by a hysteretic magnetization versus magnetic field curve. The negative field sets the bit to spin-down, the positive field sets the bit to spin-up, and the bit is interrogated at the zero-field. For a two-terminal molecular electronic switch, the variables "field" and "magnetization" should be replaced by "voltage" (V) and "current" (I). Most molecular junctions will not exhibit a hysteretic I-V response, and designing such a response into the molecule is a synthetic challenge. Our approach is to use mechanically interlocked molecules in the form of [2]catenanes (*10*) that undergo a reversible circumrotational motion of one of the rings through the cavity of the other ring upon oxidation and subsequent reduction. In this case, the voltage required to mechanically switch the molecule is the ionization energy of the molecule plus an activation barrier to ionization.

The preparation of monolayers, composed of a mixture of cyclobis(paraquat-*p*-phenylene) tetrakis(hexafluorophosphate) on its own (or as one of the components of the [2]catenanes) and the anchor phospholipid dimyristoylphosphatidic acid (DMPA) as its monosodium salt dissolved in $CHCl_3$/MeOH (3/1), has been described previously (*11*). Langmuir monolayers were prepared on an aqueous (18.2-megohm H_2O) subphase of a Langmuir-Blodgett (LB) trough (type 611D, Nima Technology, Coventry, UK). The PF_6^- salts of the tetracationic cyclophane and the two [2]catenanes incorporating it were dissolved in MeCN. Immediately before spreading, the DMPA and cyclophane/catenane solutions were mixed to yield a molar ratio of 6:1. For all Langmuir films, excepting the eicosanoic acid control (*12*), the compounds were deposited onto the aqueous subphase at 20°C and allowed to equilibrate for 30 min before transfer to the patterned substrates (*13*). The fabrication of molecular sandwich tunneling junctions from LB monolayers has been described previously (*4*). In the present work, the bottom electrodes were 7-μm-wide n-type poly-Si (resistivity of 0.02 ohm·cm). Typically, poly-Si films formed by direct chemical vapor deposition (CVD) growth onto SiO_2 are neither smooth nor defect-free. However, amorphous Si films can be very smooth (*14*), and so, amorphous Si was used as a starting point for the fabrication of smooth poly-Si electrodes. This many step process was critical for achieving a high (effectively 100%) device yield (*15*). After LB-monolayer deposition (*16*), 10-μm-wide top electrodes (50 Å Ti followed by 1000 Å Al) were deposited onto the LB film using electron-beam evaporation through a shadow mask. The dimensions of the bottom and top electrodes were 7 and 10 μm, respectively. Except where noted, we measured devices in air at room temperature, using a shielded probe station with coaxial probes. Bias voltages were applied to the poly-Si electrode, and the top electrode was connected to ground through a current preamplifier (model 1211, DL Instruments, Ithaca, New York).

With a few exceptions, the operational characteristics of our solid state devices were consistent with the known (*7*) solution-phase mechanism of the [2]catenane (Fig. 1A). This compound, whose template-directed synthesis has been described previously (*7*), consists of a tetracationic cyclophane that incorporates two bipyridinium units, interlocked with a crown ether containing a tetrathiafulvalene (TTF) unit and a 1,5-dioxynaphthalene ring system (NP) located on opposite sides of the crown ether. The switching mechanism is illustrated in Fig. 1B. The ground state "co-conformer" (*17, 18*) [A^0] of this [2]catenane has the TTF unit located inside the cyclophane. Upon oxidation, the TTF unit becomes positively charged, and the Coulombic repulsion between TTF^+ and the tetracationic cyclophane causes the crown

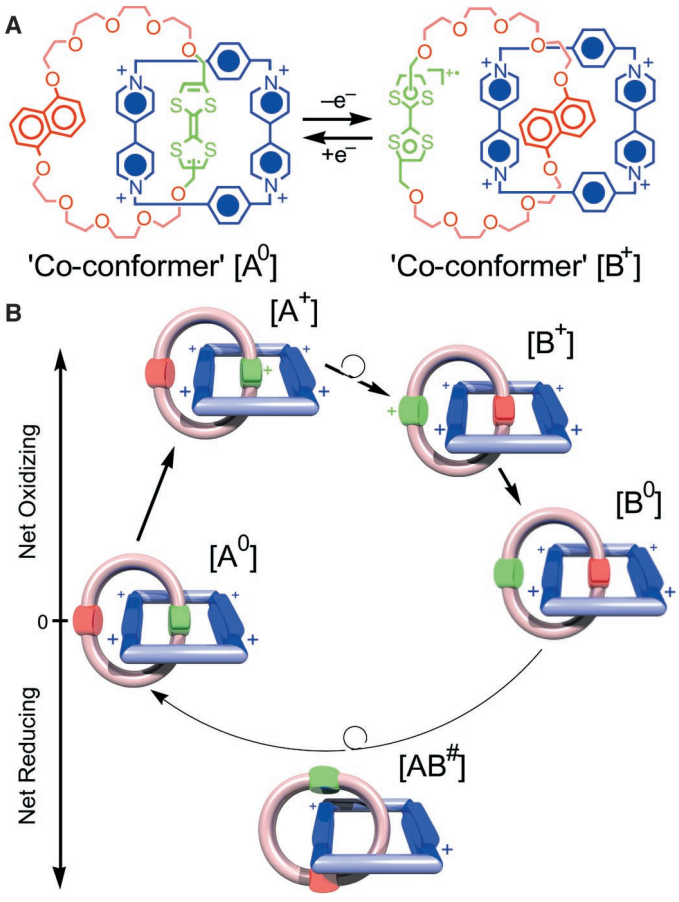

Fig. 1. (**A**) Molecular drawing of the bistable [2]catenane used in this work. The voltage-driven circumrotation of co-conformer [A^0] to co-conformer [B^+] is the basis of the device. (**B**) Proposed mechanochemical mechanism for the operation of the device. Co-conformer [A^0] represents both the ground-state structure of the [2]catenane and the "switch open" state of the device. When the [2]catenane is oxidized (by applying a bias of –2 V), the TTF groups (green) are ionized and experience a Coulomb repulsion with the tetracationic cyclophane (blue), resulting in the circumrotation of the ring and the formation of co-conformer [B^+]. When the voltage is reduced to a near-zero bias, the co-conformer [B^0] is formed, and this represents the "switch closed" state of the device. Partial reduction of the cyclophane (at an applied bias of +2 V) is necessary to regenerate the [A^0] co-conformer. For simplicity of presentation, a $2e^-$ reduction step is shown, but the actual number of electrons was not measured, and so, the reduced co-conformer [$AB^{\#}$] is indicated with an unknown oxidation state.

Department of Chemistry and Biochemistry, University of California at Los Angeles, 405 Hilgard Avenue, Los Angeles, CA 90095–1569, USA.

*To whom correspondence should be addressed. E-mail: stoddart@chem.ucla.edu (J.F.S.) and heath@chem.ucla.edu (J.R.H.)

ether to circumrotate to give co-conformer [B^+], which will reduce back to [B^0] when the bias is returned to 0 V. This bistability is the basis of this device. The energy gap between the highest occupied and lowest unoccupied molecular orbitals for co-conformer [B^0] must be narrower in energy than the corresponding gap in co-conformer [A^0], implying that, in a solid state device, tunneling current through the junction containing [B^0] will be greater. Thus, this co-conformer represents the "switch closed" state, and the ground state co-conformer [A^0] represents the "switch open" state.

Various measurements of the *I-V* hysteresis of the device are shown in Fig. 2, A to C, and Fig. 2D illustrates cycling of the device. Both the forward and reverse bias traces (Fig. 2A) cross zero current at zero voltage, indicating that the switching of the device is not related to a charge storage (capacitive) effect. Perhaps the "cleanest" experiment for probing the hysteresis of the device is to send a series of "write" voltage pulses to the device, such as –2.0, –1.9, –1.8 V, . . ., 1.9, 2.0, 1.9, 1.8 V, . . ., –2.0 V. After each write pulse, the device is read at a constant small (nonperturbing) voltage. In such an experiment, the hysteresis is recorded at a single voltage, and effects such as device capacitance are canceled out. For ferroelectric sandwich devices, this measurement is akin to generating a "remnant polarization" curve (*19*). For the present devices, we refer to this experiment as a remnant molecular signature, and we show such a measurement in Fig. 2C. This remnant molecular signature does bear similarities to the hysteresis loop of a ferromagnet.

In the solution phase, the [2]catenane exhibits only a slight hysteresis, especially when compared to the solid state device. To understand the differences between the solution-phase and solid state cycling of this molecule, it is important to consider the nature of the solid state electrochemical junction.

The device consists of the [2]catenane monolayer (*11*) isolated from both electrodes by tunneling barriers. This geometry has two implications for the operation of the device. The first implication relates to the nature of the redox chemistry that can occur within the junction. A 1- to 1.5-nm-thick SiO_2 layer exists between the [2]catenane and the poly-Si electrode, and the long alkyl chain phospholipid counterions separate the [2]catenane from the top Ti/Al electrode. In such an asymmetric device, one of the tunnel barriers will be the limiting barrier for current flow. At either positive or negative bias, it is possible to tunnel through both filled and empty molecular states, and so, one must look to the symmetry of the device to understand the redox chemistry of the junction. Consider current flowing from an electrode through a thick tunnel barrier onto a molecule and then being drained away through a thin barrier to the second electrode. For the case of the filled states, the molecule must be oxidized before current can flow through the thick barrier. Thus, oxidation of the molecule is fast (current flow through the thin barrier), but charge neutralization of the oxidized molecule (current flow through the thick barrier) is slow, and the molecule spends a relatively large amount of time in its oxidized form. Similarly, that same molecule would spend substantially less time in its reduced form. Thus, current flow in this electronic configuration is "net oxidizing," whereas the opposite bias is "net reducing." In our devices, the SiO_2 barrier is current limiting, implying that negative bias is net oxidizing and positive bias is net reducing.

The devices cycled reproducibly only if they were opened at voltages greater than +2 V and closed at voltages less than –1.5 V, implying that both oxidation and reduction are critical for device switching. Starting with co-conformer [A^0] in Fig. 1B, the state of the switch was read by measuring the junction resistance R_o at +0.1 V. Application of a bias of −2 V to the junction creates [A^+], which undergoes circumrotation to give [B^+]. Subsequent reduction of the bias generates [B^0], and the device state again can be read by measuring the junction resistance R_c at +0.1 V. A bias of +2 V is then applied to the device. We postulate that at least a partial reduction of the tetracationic cyclophane enables the transformation of [B^0] back to [A^0]. When the junction resistance is read again at +0.1 V, we find the original value (to ±10%) of R_c, which corresponds to a junction containing [A^0] co-conformers. This sequence of events constitutes one period of the complete cycle (Fig. 2B). The last step, which leads to the regeneration of [A^0], involves circumrotation of the interlocked rings with

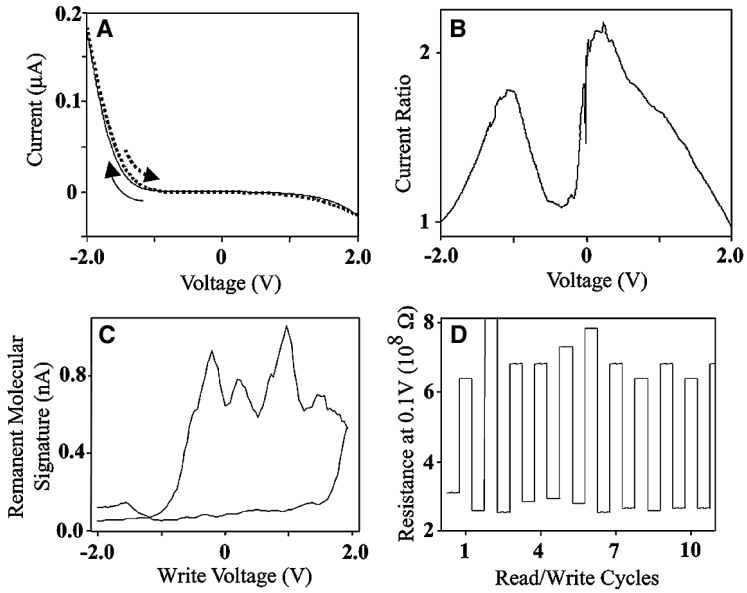

Fig. 2. (**A**) *I-V* hysteresis loop of one of the devices, as measured at 291 K. The current varied by about four decades (from tenths of mA to hundreds of pA) over the range of the voltage scan. The diode effect originates largely from the two different electrode materials. In (**B**), the structure of this hysteresis is highlighted by plotting the current ratio of the forward divided by the reverse bias scans. (**C**) The remnant molecular signature of the device, measured by varying the write voltage in 40-mV steps and by reading the device at –0.2 V. (**D**) The switching operation of this device, as measured at 291 K. The junction resistance was read at a bias of +0.1 V as the device was alternately opened at +2 V and closed at –2 V. The devices did not appear to age as a consequence of repeated cycling. However, our (unpackaged) devices ceased to operate after a period of 2 to 3 months.

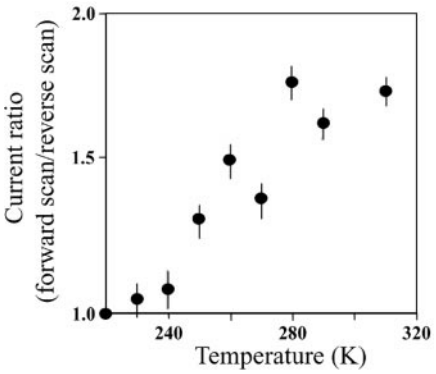

Fig. 3. Plotting the negative bias peak in the hysteresis ratio versus temperature represents the temperature dependence of the molecular switch. Near 220 K, the switching of the device is quenched, indicating that the mechanism of the device operation has at least one thermally activated step. Error bars represent the noise in the *I-V* measurements.

respect to one another within the [2]catenane. We hypothesize that the energy barrier to this relative motion is lowered by decreasing the Coulombic interactions between the positively charged [2]catenane and the phospholipid counterions. Nevertheless, this step should still be an activated process. Thus, whereas the [A^+] to [B^+] circumrotational process is voltage activated, the regeneration of [A^0] is thermally and voltage activated. This mechanism is consistent with temperature-dependent measurements (Fig. 3), which indicate that the overall cycling of the switches has at least one thermally activated component and is quenched near 200 K.

The second implication of our double tunnel barrier device geometry relates to the voltage-dependent electronic signatures of the [2]catenane. When a charged molecule is placed at some distance r from a conducting surface, the conducting surface exhibits a polarization response to the charged molecule, which leads to an image charge of opposite sign at a distance of $-r$ within the electrode (*20*). This response results in a Coulomb stabilization of the charged molecule that scales as $e^2/\varepsilon r$, where e is the fundamental unit of charge and ε is the dielectric constant of the tunnel barrier separating the charged molecule and the electrode. The net effect is that the energy levels of the molecule are pulled toward the Fermi levels of the electrodes, and the electronic signatures of the molecule can therefore be masked. The purpose of our tunnel barriers is to minimize this effect by removing the molecules from the surface of the electrodes. At the same time, however, the tunnel barriers must still be relatively thin or current will not flow through the device. Thus, we expect that the molecules will still be somewhat coupled to the electrodes through image charges. In our device, one of the electrodes is n-doped poly-Si. As temperature is reduced, the charge carriers in the electrode will begin to "freeze out." The polarizability of that electrode will decrease, and the electronic states of the [2]catenanes will decouple from that electrode. This response is, in fact, what we see. In Fig. 4, the peak position, taken from the negative bias portion of the hysteresis ratio (Fig. 2B), is plotted versus temperature. As temperature is reduced from 310 to 230 K, the hysteresis peak shifts away from the Fermi level of the electrodes by ~0.4 V. This observation is further evidence for the proposed mechanochemical switching mechanism described above.

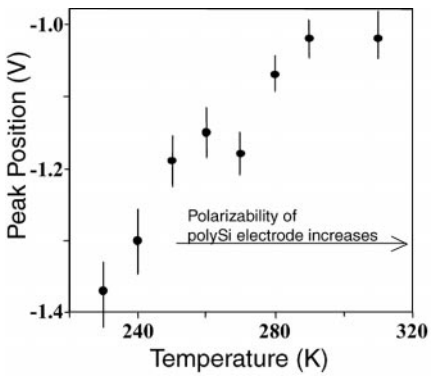

Fig. 4. The voltage position of the negative bias peak in the *I-V* hysteresis ratio is plotted as a function of temperature. As temperature increases, the hysteresis features shift toward the Fermi levels of the electrodes (zero bias), indicating the presence of image charges in the electrodes that tend to mask the molecular electronic energy levels. At low temperature, the polarizability of the poly-Si decreases, and the electronic states of the molecule will decouple from that electrode (and shift away from zero bias). Minimizing the coupling between the molecules and the electrodes while maximizing the current flow through the device is a key aspect in the design of a solid state molecular electronic switch. Error bars represent the uncertainties in determining the peak positions.

Control experiments were performed by substituting the following for the bistable [2]catenane layer in the devices: (i) eicosanoic acid; (ii) DMPA as its monosodium salt; (iii) the tetracationic cyclophane, namely, cyclobis(paraquat-*p*-phenylene), anchored with DMPA counterions (*21*); and (iv) a monostable degenerate [2]catenane (*11*), wherein the same tetracationic cyclophane is interlocked with bis-*p*-phenylene-34-crown-10 (BPP34C10) and is also anchored with DMPA counterions. Although a very small amount of hysteresis (<1% of the principal devices) was observed in the *I-V* curves of some of these controls, it decayed quickly over time and was attributable to a residual capacitance. The principal devices could be operated for more than a month under ambient conditions and without packaging.

These bistable devices exhibited robust operation under ambient conditions. We intermittently cycled some of these devices a few hundred times over a period of 2 months without observing substantial changes in their properties. The junction resistance between the closed and open states of the device differs by approximately a factor of 4, implying that these devices may, upon further engineering, be useful as memory devices but are unlikely to be important for logic applications.

References and Notes

1. A. Aviram and M. R. Ratner, *Chem. Phys. Lett.* **29**, 277 (1974).
2. R. M. Metzger, *J. Mater. Chem.* **10**, 55 (2000).
3. J. Chen, M. A. Reed, A. M. Rawlett, J. M. Tour, *Science* **286**, 1550 (1999).
4. C. P. Collier *et al.*, *Science* **285**, 391 (1999).
5. E. W. Wong *et al.*, *J. Am. Chem. Soc.* **122**, 5831 (2000).
6. M. Asakawa *et al.*, *Angew. Chem. Int. Ed. Engl.* **37**, 333 (1998).
7. V. Balzani *et al.*, *J. Org. Chem.* **65**, 1924 (2000).
8. M. Asakawa *et al.*, *Eur. J. Org. Chem.* **1999**, 985 (1999).
9. J. R. Heath, P. J. Kuekes, G. S. Snider, R. S. Williams, *Science* **280**, 1716 (1998).
10. For an example of partial circumrotation of interlocked molecular rings in a [2]catenane in the solid state, see work by T. Gase *et al.* [*Adv. Mater.* **11**, 1303 (1999)].
11. C. L. Brown *et al.*, *Langmuir* **16**, 1924 (2000).
12. For the eicosanoic acid control, the subphase was held at 25°C, and the monolayer was compressed at 10 cm^2/min to a surface pressure of 1.0 mN/m and then at 2.0 cm^2/min to the deposition pressure of 25.0 mN/m.
13. These Langmuir monolayers were compressed at 10 cm^2/min to a surface pressure of 1.0 mN/m, at 5 cm^2/min to a surface pressure of 14.0 mN/m, and, finally, at 2 cm^2/min to the deposition pressure of 30 mN/m. The monolayers were then deposited as LB films onto the electrode-patterned poly-Si substrates on the upstroke at 1 mm/min, after equilibrating for 3 min. The monolayers transferred at a stoichiometry of [2]catenane^{4+} + 6Na^+ + 4 PF_6^- + 6 $DMPA^-$ and the following areas per molecular complex: (i) 125 $Å^2$ for TTF/NP-[2]catenane, (ii) 160 $Å^2$ for the parent BPP34C10-[2]catenane, and (iii) 90 $Å^2$ for the cyclophane on its own.
14. T. Kamins, *Polycrystalline Silicon for Integrated Circuit Applications* (Kluwer Academic, Boston, 1988), chap. 4.
15. The poly-Si electrodes were fabricated as follows. Low-pressure SiH_4 CVD was used to deposit 1500 Å of amorphous Si onto 1100 Å of SiO_2 on a Si<100> wafer at 525°C. The film was exposed to air at room temperature for several minutes to form a passivating SiO_2 layer and then crystallized under N_2 at 650°C. Poly-Si films were implanted with 55-keV P^+ ions, and a 1-μm film of SiO_2 was grown by CVD to prevent outgassing of the phosphorus. The dopant P atoms were activated at 1000°C, and then, a 6:1 mixture of NH_4F(aq):HF(aq) was used to etch away the SiO_2. Electrodes were patterned by using standard photolithography techniques.
16. LB films were deposited onto nonpatterned substrates of identically cleaned SiO_2 and poly-Si, and contact angles of H_2O (18.2 megohms, millipure) on the substrate were measured as a check of monolayer quality, with the following results: cleaned SiO_2 (0°), cleaned poly-Si (11°), eicosanoic acid on SiO_2 (75°), eicosanoic acid on poly-Si (72°), TTF/NP-[2]catenane on SiO_2 (108°), and TTF/NP-[2]catenane on poly-Si (108°). The subphase for all monolayer transfers was 6.4 mM $CdCl_2$(aq), adjusted to pH 8.5 with NaOH(aq).
17. We advocate the term "co-conformation" to describe the different three-dimensional spatial arrangements of the components of mechanically interlocked molecules like catenanes. Here, we use the term "co-conformer" in reference to the [A^0] and [B^+] structures, recognizing that, strictly speaking, because of their different redox characteristics, they are not isomers.
18. M. Fyfe *et al.*, *Angew. Chem. Int. Ed. Engl.* **36**, 2068 (1997).
19. M. E. Lines and A. M. Glass, *Properties and Applications of Ferroelectrics and Related Materials* (Clarendon, Oxford, 1977), p. 103.
20. S. M. Sze, Ed., *Physics of Semiconductor Devices* (Wiley, New York, ed. 2, 1981).
21. R. C. Ahuja *et al.*, *Langmuir* **9**, 1534 (1993).

22. This research was supported by the Defense Advanced Research Projects Agency and by the NSF. C.P.C. is an employee of the Hewlett-Packard Company. We acknowledge T. Kamins (Hewlett-Packard) for useful advice in preparing the poly-Si electrodes and the staff at the University of California at Los Angeles (UCLA) Nanoelectronics Research Facility for helpful advice in device fabrication. A. Pease (UCLA) designed the artwork used in Fig. 1.

16 February 2000; accepted 30 June 2000